N-Hydroxy-4-aminobiphenyl-DNA Binding in Human *p53* Gene: Sequence Preference and the Effect of C5 Cytosine Methylation†

Zhaohui Feng,‡ Wenwei Hu,‡ William N. Rom,§ Frederick A. Beland,|| and Moon-shong Tang*,‡,§,⊥

Departments of Environmental Medicine, Medicine, and Pathology, New York University Medical Center, Tuxedo, New York 10987, and Division of Biochemical Toxicology, National Center for Toxicological Research, Jefferson, Arkansas 72079

Received January 31, 2002; Revised Manuscript Received March 22, 2002

ABSTRACT: 4-Aminobiphenyl (4-ABP) is a major etiological agent for human bladder cancer. Metabolically activated 4-ABP is able to interact with DNA to form adducts that may induce mutations and initiate carcinogenesis. Thirty to sixty percent of bladder cancer has a mutation in the tumor suppressor *p53* gene, and the mutational spectrum bears unique features. To date the DNA binding spectrum of 4-ABP in the *p53* gene is not known due to the lack of methodology to detect 4-ABP-DNA adducts at nucleotide sequence level. We have found that UvrABC nuclease, a nucleotide excision repair complex isolated from *Escherichia coli*, is able to incise specifically and quantitatively DNA fragments modified with *N*-hydroxy-4-aminobiphenyl (N-OH-4-ABP), an activated intermediate of 4-ABP. Using the UvrABC nuclease incision method, we mapped the binding spectrum of N-OH-4-ABP in DNA fragments containing exons 5, 7, and 8 of the human *p53* gene and also determined the effect of C5 cytosine methylation on N-OH-4-ABP-DNA binding. We found that codon 285, a mutational hotspot at a non-CpG site in bladder cancer, is the preferential binding site for N-OH-4-ABP. We also found that C5 cytosine methylation greatly enhanced N-OH-4-ABP binding at CpG sites, and that two mutational hotspots at CpG sites, codons 175 and 248, became preferential binding sites for N-OH-4-ABP only after being methylated. These results suggest that both the unique DNA binding specificity of 4-ABP and cytosine methylation contribute to the mutational spectrum of the *p53* gene in human bladder cancer.

The aromatic amine 4-aminobiphenyl (4-ABP;[1] Figure 1), a component in cigarette smoke, an environmental and industrial contaminant, is believed to be a major etiological agent of human bladder cancer (*1, 2*). Metabolically activated electrophilic derivatives of 4-ABP are able to interact with DNA to form adducts, which have been found to correlate with bladder carcinogenesis in experimental animals (*3*−*6*) and humans (*7*−*11*). The predominant DNA adduct induced by 4-ABP in vivo is *N*-(2′-deoxyguanosin-8-yl)-4-ABP (80%); minor amounts of *N*-(2′-deoxyadenosin-8-yl)-4-ABP (15%) and 3-(2′-deoxyguanosin-N^2-yl)-4-ABP (5%) are also formed (*3, 12;* Figure 1). 4-ABP is metabolized primarily in the liver, where it is oxidized to *N*-hydroxy-4-ABP (N-OH-4-ABP; Figure 1). N-OH-4-ABP enters the circulation, is filtered through the kidney, and is transported to the urinary bladder, where upon reabsorption it can react with DNA either directly or upon *O*-esterification (*13, 14*).

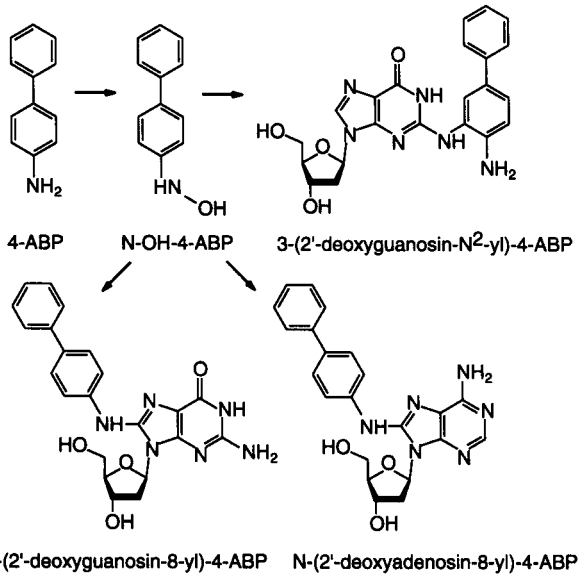

FIGURE 1: Chemical structures of 4-ABP, N-OH-4-ABP, *N*-(2′-deoxyguanosin-8-yl)-4-ABP, *N*-(2′-deoxyadenosin-8-yl)-4-ABP, and 3-(2′-deoxyguanosin-N^2-yl)-4-ABP.

In humans, 30−60% of bladder cancers have mutations in the tumor suppressor *p53* gene (*15, 16*). The *p53* mutational spectrum in bladder cancer is significantly dif-

† This research was supported by NIH Grants ES03124, ES08389, ES00260, ES10344, MO100096 (M.T.), and CA86137 (W.N.R.).

* To whom correspondence should be addressed at the Department of Environmental Medicine, New York University Medical Center, Tuxedo, NY 10987. E-mail: tang@env.med.nyu.edu. Telephone: 845-731-3585. Fax: 845-351-2385.

‡ Department of Environmental Medicine, New York University Medical Center.

§ Department of Medicine, New York University Medical Center.

|| Division of Biochemical Toxicology, National Center for Toxicological Research.

⊥ Department of Pathology, New York University Medical Center.

[1] Abbreviations: 4-ABP, 4-aminobiphenyl; N-OH-4-ABP, *N*-hydroxy-4-aminobiphenyl; BPDE, benzo[*a*]pyrene diol epoxide; PAHs, polycyclic aromatic hydrocarbons; BCDE, benzo[*g*]chrysene diol epoxide; AFB1-DE, aflatoxin B_1 8,9-diol epoxide; NAAAF, *N*-acetoxy-2-acetylaminofluorene; SAM, *S*-adenosylmethionine; bp, base pair.

10.1021/bi020093s CCC: $22.00
Published on Web 04/24/2002

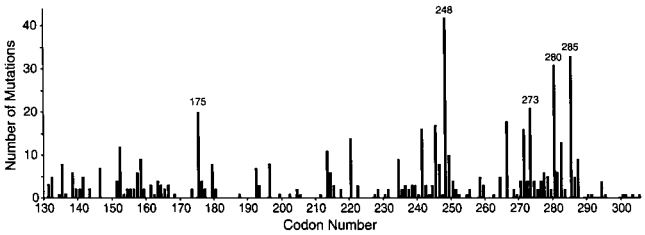

FIGURE 2: Mutational spectrum in exons 5−8 in the *p53* gene in human bladder cancer. The numbers were obtained from the June 2001 update of the International Agency for Research on Cancer (IARC) T*P53* mutation database with a total number of 627 mutations (http//:www-p53.iarc.fr/p53DataBase.htm). The labeled codons have a mutation frequency more than 3% of total 627 mutations.

ferent from other cancers: the mutational frequency is more evenly distributed along the *p53* gene, and the mutations do not bias at methylated CpG sites. Most notably, it has mutational hotspots at codons 280 and 285, two non-CpG sites, besides codons 175, 248, and 273 (Figure 2). Codons 175, 248, and 273 contain CpG sites and are common mutational hotspots in many human cancers; however, codons 280 and 285 contain no CpG sites and are mutational hotspots unique for bladder cancer and cancers of other urinary organs [International Agency for Research on Cancer (IARC) *P53* mutation database].

More than 200 mutated codons of the *p53* gene have been identified in human cancers, and the mutation spectra often seem to bear the signature of the etiological agents (*15*−*18*). Smoking-associated lung cancer is a notable example. In lung cancer of cigarette smokers, *p53* gene mutations are concentrated at several methylated CpG sites, specifically at codons 157, 158, 175, 245, 248, 273, and 282 (*15*−*18*). We have previously found that benzo[*a*]pyrene diol epoxide (BPDE), a major metabolite of the cigarette smoke carcinogen benzo[*a*]pyrene, and diol epoxides from other polycyclic aromatic hydrocarbons (PAHs) preferentially form DNA adducts at methylated CpG sites corresponding to the aforementioned mutational hotspots observed in human lung cancer of cigarette smokers (*19*−*21*). We have also shown that methylation at C5 of cytosine greatly enhances the binding of PAH diol epoxides at CpG sites in the *p53* gene, indicating that methylation is the major cause for preferential adduct formation at CpG sites in the human *p53* gene (*22*). These results suggest that the initial DNA adduct distribution in the *p53* gene contributes greatly to the mutation spectrum in human tumors. If this is the case, then it is plausible to hypothesize that the unique *p53* mutational hotspots in bladder cancer result from the unique DNA binding of 4-ABP in the *p53* gene since 4-ABP is a major etiological agent for bladder cancer. To date, this relationship has not been explored due to lack of methodology for detecting the 4-ABP-DNA binding spectrum at the nucleotide sequence level. This motivated us to develop a method to detect the distribution of 4-ABP-DNA adducts at the sequence level.

It has been well established that the nucleotide excision complex UvrABC nuclease isolated from *Escherichia coli* is able to incise quantitatively and specifically a variety of DNA damage ranging from helix destabilizing adducts to helix stabilizing adducts. This UvrABC nuclease incision method has been applied successfully to determine the sequence specificity of bulky chemical carcinogen-DNA adducts and their repair (*19*, *23*−*29*). In this report, we have characterized the mode of incision of UvrABC toward DNA modified with N-OH-4-ABP. We have found that UvrABC nuclease is able to incise N-OH-4-ABP-DNA adducts quantitatively and specifically. Using this method, we have determined the N-OH-4-ABP-DNA binding spectrum in exons 5, 7, and 8 of the human *p53* gene. We also investigated the effect of cytosine methylation at CpG sites upon the binding of N-OH-4-ABP in the *p53* gene.

MATERIALS AND METHODS

Materials. N-OH-4-ABP was synthesized according to the method described previously (*30*). BPDE was purchased from Chemsyn Science Laboratories (Lenexa, KS). *Hif*I restriction enzyme, T4 polynucleotide kinase, DNA polymerase (Klenow fragment), and Taq DNA polymerase were purchased from Promega (Madison, WI). *Sss*I methylase and *S*-adenosylmethionine (SAM) were obtained from New England Biolabs (Beverly, MA). [α-^{32}P]dATP and [γ-^{32}P]-ATP (specific activity ~3000 Ci/mmol) were purchased from NEN (Boston, MA). Primers were synthesized by Midland Certified Reagent Co. (Midland, TX).

DNA Fragment Isolation and ^{32}P-End-Labeling. A 187 bp 5′-^{32}P-end-labeled DNA exon 7 fragment was obtained by amplification of an exon 7 region from a plasmid containing the human *p53* gene (pAT153*p53*π; obtained from L. Crawford and S. P. Tuck, Imperial Cancer Fund Laboratories, London, U.K.) using two oligonucleotide primers, 5′-GCACTGGCCTCATCTTGGGCCTG-3′ and 5′-CACAG-CAGGCCAGTGTGCAGGGT-3′, with the former labeled at the 5′ end with [γ-^{32}P]ATP according to the method described previously (*29*). The 5′-^{32}P-end-labeled DNA fragment was purified by electrophoresis on an 8% polyacrylamide gel.

To obtain a 3′-^{32}P-end-labeled DNA fragment containing exon 7 of the *p53* gene, the 187 bp DNA fragment was amplified as described above using two nonlabeled primers. The fragment was digested with *Hif*I restriction enzyme, and a 141 bp product was isolated from a 2% agarose gel. The fragment was then 3′-labeled with [α-^{32}P]dATP according to the previously described method (*29*). The resulting 141 bp fragment, singly 3′-end-labeled, was purified as described above. A 247 bp 5′-end-labeled DNA fragment containing exon 5 of the *p53* gene and a 210 bp 5′-end-labeled DNA fragment containing exon 8 of the *p53* gene were amplified from pAT153*p53*π plasmid and purified as described above. The primers used for amplification of exon 5 were 5′-TGCCCTGACTTTCAACTCTGTCTCC-3′ and 5′-TCTCTC-CAGCCCCAGCTGCTCAC-3′, with the former being 5′-^{32}P-end-labeled; and those for exon 8 were 5′-ACT-GCCTCTTGCTTCTCTTTTCCTATCC-3′ and 5′-CTTG-GTCTCCTCCACCGCTTCTTG-3′, with the former being 5′-^{32}P-end-labeled.

5-C Cytosine Methylation at CpG Sites. The 5′-^{32}P -end-labeled DNA fragments were subjected to *Sss*I methylase treatment in the presence of SAM, according to manufacturer's instructions, to methylate all cytosines at CpG sites.

N-OH-4-ABP and BPDE Modification of DNA Fragment. N-OH-4-ABP was dissolved in argon-purged ethanol at a concentration of 1 mg/mL to prepare a stock solution. DNA fragments were dissolved in 90 μL of 10 mM sodium citrate

buffer (pH 5.0), extensively purged with argon, mixed with 10 μL of different concentrations of N-OH-4-ABP solution, and incubated at 37 °C for 8 h. Noncovalently bond decomposition products were removed by repeated phenol and diethyl ether extractions, and DNA fragments were ethanol-precipitated, washed with 70% ethanol, and dried under vacuum (*30*). BPDE was dissolved in dimethyl sulfoxide at a concentration of 1 mg/mL. DNA fragments were dissolved in 90 μL of TE buffer [10 mM Tris-HCl and 1 mM EDTA (pH 7.8)], mixed with different amounts of BPDE, and incubated at 25 °C for 2 h (*22*). The DNA was purified as described above.

Purification of UvrA, UvrB, and UvrC Proteins. The UvrA, UvrB, and UvrC proteins were isolated from the *E. coli K12* strain CH296, which carried plasmids pUNC 45 (*uvrA*), pUNC21 (*uvrB*), or pDR3274 (*uvrC*) (*31*). These plasmids and strain CH296 were kindly provided by Dr. A. Sancar, University of North Carolina, Chapel Hill, NC. The purification procedures were the same as previously described (*29, 32*).

UvrABC Incision Assay of DNA Fragments. The adduct distribution at various positions on the DNA fragments was mapped by the UvrABC nuclease incision method (*27*). In brief, a 6-fold molar excess of UvrABC nuclease was added to carcinogen-modified DNA fragments in a reaction buffer containing 100 mM KCl, 1 mM ATP, 10 mM $MgCl_2$, 10 mM Tris-HCl (pH 7.5), and 1 mM EDTA. The reactions were carried out at 37 °C for various times and were stopped by phenol and ether extractions followed by ethanol precipitation of the DNA.

DNA Sequencing, Gel Electrophoresis, and Autoradiography. Individual 5′- and 3′-^{32}P-end-labeled DNA fragments were sequenced by the Maxam−Gilbert chemical cleavage method (*33*). The ^{32}P-labeled DNA fragments, with or without UvrABC enzyme treatments, were suspended in sequencing tracking dye (80% v/v deionized formamide, 0.1% xylene cyanol, and 0.1% bromophenol blue), heated at 90 °C for 5 min, and separated by electrophoresis in 8% denaturing polyacrylamide gels. The gels were dried, and initially exposed to a phosphor screen and then to Kodak films. The intensity of the bands was determined by a PhosphorImager (Cyclone, Packard).

RESULTS

N-OH-4-ABP-DNA Adducts Are Sensitive to UvrABC Incision. It is well established that the UvrABC nuclease will incise various types of DNA damage (*23*−*29*). The UvrABC incision induced by damaged DNA is characterized by dual incisions; the enzyme incises six to eight bases 5′ and three to five bases 3′ of the damaged base(s) (*23*−*27*). To test whether UvrABC nuclease is able to recognize and incise N-OH-4-ABP-DNA adducts, DNA fragments labeled with ^{32} P at either the 5′ or the 3′ end were treated with different concentrations of N-OH-4-ABP and then reacted with UvrABC nuclease. Figure 3 shows the results of electrophoretic separations in a denaturing polyacrylamide gel of the UvrABC-treated DNA. When 5′-^{32}P-end-labeled DNA fragments modified with N-OH-4-ABP were reacted with UvrABC nuclease, the general cutting bands corresponded to Maxam and Gilbert purine reaction ladders, but were 7 nucleotides smaller (Figure 3A). When 3′-^{32}P-end-labeled DNA modified with N-OH-4-ABP was used as substrate, the UvrABC reaction also generated bands corresponding to Maxam−Gilbert purine reaction ladders, but bands were 4 nucleotides smaller (Figure 3B). These results suggest that UvrABC makes dual incisions 7 bases 5′ and 4 bases 3′ of N-OH-4-ABP modified purine. These results are consistent with the published results showing that purified UvrABC typically makes two incisions, one being 6−8 bases 5′ of the damaged base and the other being 3−5 bases 3′ of a damaged base (*23*−*27*).

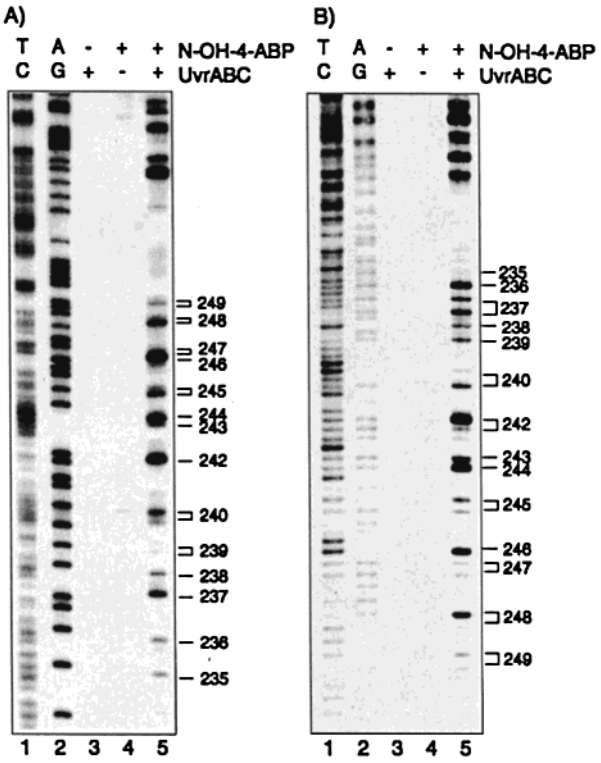

FIGURE 3: UvrABC incision of N-OH-4-ABP-modified DNA fragments. (A) 5′-^{32}P-end-labeled 187 bp fragments containing exon 7 of the human *p53* gene were modified (lanes 4 and 5) or not modified with 30 μM N-OH-4-ABP (lane 3) and then reacted (lanes 3 and 5) or not reacted with UvrABC nuclease (lane 4). (B) 3′-^{32}P-end-labeled 141 bp fragments containing exon 7 of the human *p53* gene were modified (lanes 4 and 5) or not modified with 30 μM N-OH-4-ABP (lane 3) and then reacted (lanes 3 and 5) or not reacted with UvrABC nuclease (lane 4). The carcinogen modifications, UvrABC nuclease reactions, and sequencing gel electrophoresis are described in the text. The codon numbers corresponding to the UvrABC incision bands are depicted on the right side of the panels. TC and AG are the Maxam−Gilbert sequencing reactions.

UvrABC Nuclease Incises N-OH-4-ABP-DNA Adducts Quantitatively, and the Incisions Are Sequence-Independent. The intensities of N-OH-4-ABP-induced UvrABC incision bands shown in Figure 3 vary at different sequences; this could be due to different affinities of N-OH-4-ABP modification at different sequences or to sequence-dependent incision by UvrABC nuclease. Since DNA polymerase and ligase are not present in the UvrABC incision reaction, the incision must be an irreversible reaction (*23*−*25*). As such, it is possible to distinguish between sequence-specific modification as compared to sequence-specific incision by a kinetic analysis. In our incubations, the molar ratio of UvrABC protein to substrate DNA was 6, and the UvrABC nuclease was still active after a 90 min incubation (data not shown). If the UvrABC nuclease incision had a sequence

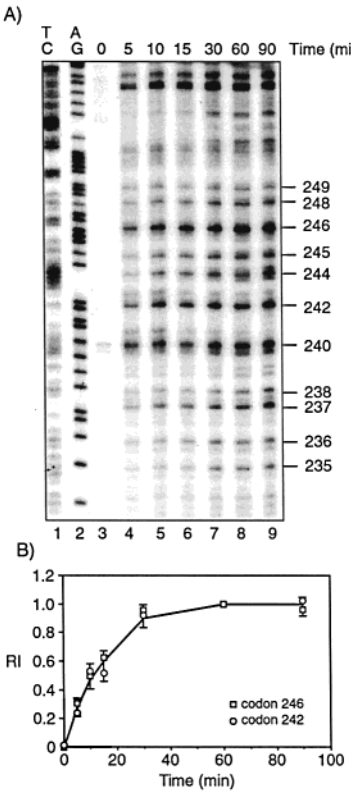

FIGURE 4: Time course for UvrABC nuclease incision of N-OH-4-ABP-modified DNA fragments. 5′-^{32}P-end-labeled 187 bp fragments containing exon 7 of the human *p53* gene were modified with 30 μM N-OH-4-ABP and then incubated with UvrABC nuclease (lanes 3−9) for 0, 5, 10, 15, 30, 60, or 90 min. The resultant DNAs were separated in an 8% polyacrylamide denaturing gel. Eleven well-separated bands labeled with corresponding codon numbers were depicted on the right side of the panel, and were chosen for quantification. The intensity of each UvrABC incision band was quantified with a PhosphorImager. The relative band intensities (RI) were adjusted by the amount of sample applied to the gel and normalized to the band intensities at the 60 min incubation. (A) Autoradiograph and (B) the kinetics of UvrABC incision at different sequences in the N-OH-4-ABP-modified DNA fragments. The lines in the panel represent the mean value of the 11 different sequences; for clarity, only 2 sequence points are presented in the panel: the rest of the sequence points are within the lengths of the error bars.

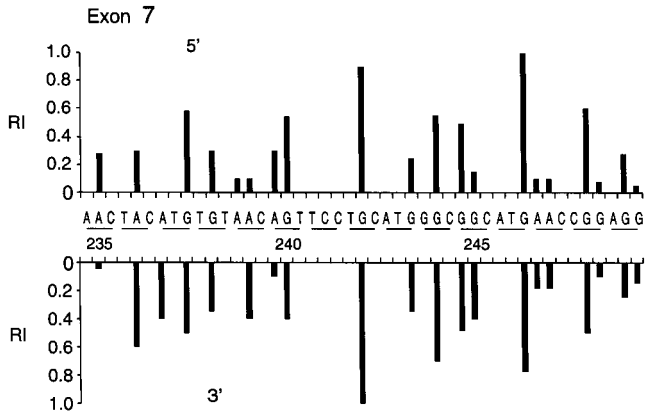

FIGURE 5: DNA binding spectrum of N-OH-4-ABP in exon 7 of the human *p53* gene. 5′-End-^{32}P-labeled (upper panel) or 3′-end-^{32}P-labeled (lower panel) DNA fragments containing exon 7 of the *p53* gene were modified with 30 μM N-OH-4-ABP, reacted with UvrABC nuclease, and then separated by gel electrophoresis as described in the text. The intensities of UvrABC incision bands in well-separated regions were quantified with a PhosphorImager. The extent of N-OH-4-ABP-DNA binding is represented by the relative intensity (RI) of UvrABC incision bands. The RI was calculated based on RI = I_j/I_{max}, where I_j is the intensity of each UvrABC incision band and I_{max} is the UvrABC incision band with the highest intensity in an autoradiograph.

preference, then the rate constants of incision at different sequences should be different. On the other hand, if the UvrABC incision had no sequence preference, then the rate constant of incision at different sequences should be similar; hence, the extent of incision at different sequences should reflect the amount of adduct formation at those sequences. A typical time course of UvrABC incision on the N-OH-4-ABP-DNA fragments is shown in Figure 4A. It is apparent that the intensities of the UvrABC incisions are a function of incubation time and reach a plateau after the same incubation time. Eleven well-separated bands, nine representing dG adducts and two representing dA adducts, were chosen for quantification. The results shown in Figure 4B demonstrate that UvrABC incises the DNA adducts in these sequences with identical kinetics and the incision reaches a plateau after 30 min of incubation. Since the molar ratio of UvrABC/DNA was 6 in these reaction conditions and because the UvrABC incision is an irreversible reaction, these data strongly suggest that the DNA sequence does not play a significant role in determining the efficiency of UvrABC incision and that the degree of UvrABC incision is proportional to the extent of 4-ABP binding. To obtain further support for this conclusion, we determined the efficiency of UvrABC incision at these sequences in the DNA fragments modified with different concentrations of N-OH-4-ABP, and found that the extent of UvrABC incision was proportional to the N-OH-4-ABP concentration (data not shown). Together, these results indicate that UvrABC nuclease incises N-OH-4-ABP-DNA adducts not only specifically but also quantitatively under our reaction conditions.

The results in Figure 5 demonstrate that the relative intensities of UvrABC cutting at the 5′- and 3′-sides of an N-OH-4-ABP-modified base are comparable, which further reflects the dual incisions of UvrABC nuclease on N-OH-4-ABP-DNA. Therefore, either 5′- or 3′-end-labeled fragments can be used for determining the N-OH-4-ABP-DNA binding spectrum. The results in Figure 5 also show that N-OH-4-ABP mainly reacts with guanine and to a much lesser extent with adenine: UvrABC incision bands corresponding to guanine residues accounted for 80% of the total intensity of the UvrABC incision bands. These results are consistent with published results that *N*-(2′-deoxyguanosin-8-yl)-4-ABP accounts for ~80% of the total adducts formed in DNA from reaction with N-OH-4-ABP (*3, 12*).

Binding Spectrum of N-OH-4-ABP Adducts in Exons 5, 7, and 8 of the Human p53 Gene. Our results show that the intensity of UvrABC incision at different sequences represents the sequence preference of N-OH-4-ABP-DNA binding; therefore, the UvrABC incision method can be used to determine the sequence selectivity of N-OH-4-ABP-DNA binding. DNA fragments containing exons 5 and 8 of the human *p53* gene were 5′-end-labeled and modified with N-OH-4-ABP. The modified DNA fragments were then incubated with UvrABC nuclease, and the resultant DNAs were gel-separated. Figure 6A shows typical autoradiographs; the quantitative results are shown in Figure 6B. N-OH-4-ABP binds significantly at codons 160, 164, 167, and 175

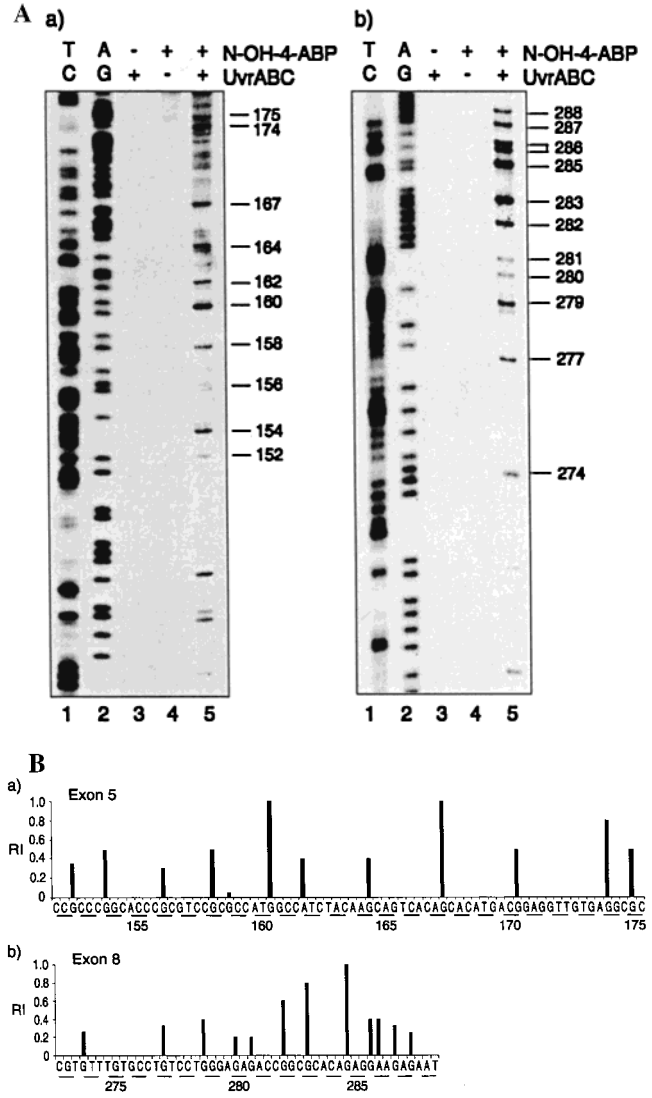

FIGURE 6: DNA binding spectrum of N-OH-4-ABP in exons 5 and 8 of the human *p53* gene. 5′-^{32}P-end-labeled DNA fragments containing exons 5 (A-a and B-a) or 8 (A-b and B-b) of the human *p53* gene were modified (lanes 4 and 5) or not modified with 30 μM N-OH-4-ABP (lane 3) and then reacted (lanes 3 and 5) or not reacted with UvrABC nuclease (lane 4). The carcinogen modifications, UvrABC nuclease reactions, and sequencing gel electrophoresis are the same as described in the text. Well-separated bands are labeled with corresponding codon numbers on the right side of the panels. The extent of N-OH-4-ABP-DNA binding is represented by the relative intensity (RI) of UvrABC incision, and the quantitation is the same as in Figure 5. TC and AG are the Maxam−Gilbert sequencing reactions. (A) Typical autoradiographs and (B) quantitation.

of exon 5; it also binds strongly at codons 282, 283, and 285 of exon 8. As noted previously, codons 242 and 246 of exon 7 are also strong binding sites of N-OH-4-ABP (Figures 3 and 5). These results demonstrate that among the five mutational hotspots in the *p53* gene in human bladder cancer, codons 285 and 248 show strong and moderate binding affinity, respectively, toward N-OH-4-ABP, while codons 175, 280, and 273 show either weak or no binding affinity toward N-OH-4-ABP.

Effect of Cytosine Methylation on N-OH-4-ABP Binding at CpG Sites. Most of the mutational hotspots in the *p53* gene in human cancer are at CpG sites; for example, more than 30% of the *p53* mutations occur at CpG sites in codons 157, 175, 245, 248, 273, and 282, although there are few exceptions, such as codon 249 in liver cancer and codons 280 and 285 in bladder cancer (*15*−*18*). Previously we have shown the preferential binding of BPDE at CpG sites that correspond to the mutational hotspots in lung cancer of smokers (codons 157, 175, 245, 248, 273, and 282) (*19*−*21*). Furthermore, C5 cytosine methylation greatly enhanced adduct formation at all CpG sites in the *p53* gene by a variety of exogenous bulky chemical carcinogens, including BPDE, benzo[*g*]chrysene diol epoxide (BCDE), *N*-acetoxy-2-acetylaminofluorene (NAAAF), and aflatoxin B_1 8,9-diol epoxide (AFB1-DE) (*22*). Since all cytosine residues at CpG sites in the coding region of the human *p53* gene are highly methylated in a variety of tissues (*34*), these findings strongly suggest that mutational hotspots at methylated CpG sites in the *p53* gene may be a consequence of preferential binding of chemical carcinogens. To determine the effect of C5 cytosine methylation on N-OH-4-ABP binding at CpG sites in the *p53* gene, we compared the binding spectra of N-OH-4-ABP and BPDE for the methylated *p53* gene. DNA fragments 5′-^{32}P-end-labeled were subjected to *Sss*I methylase treatment in the presence of SAM to methylate all cytosines at CpG sites. DNA fragments with and without methylation treatment were then modified with N-OH-4-ABP or BPDE, and the adduct distributions at various sequence positions were mapped by the UvrABC incision method. The extent of cytosine methylation was determined by Maxam−Gilbert chemical cleavage reaction (*33*). Hydrazine is unable to modify 5-C-methylated cytosines; consequently, both the 5′ and 3′ phosphodiester bonds of each methylated cytosine are refractory to piperidine hydrolysis, and no cytosine ladders are observed at methylated cytosines (*35*). Figure 7A shows that under our methylation conditions, all of the CpG sites in the DNA fragments containing exons 5, 7, and 8 sequences of the *p53* gene are methylated.

The results in Figure 7 show that cytosine methylation does enhance N-OH-4-ABP binding at almost all CpG sites in the *p53* gene by 1−2-fold, except codon 273, which remains refractory to N-OH-4-ABP binding. A greater enhancement of N-OH-4-ABP binding is seen at CpG sites of codons 175 and 248 after methylation, which turn out to be preferred binding sites of N-OH-4-ABP in exon 5 and 7, respectively (Figure 7A-a,b and 7B-a,b). Methylation also enhances N-OH-4-ABP binding at codons 245 and 282, codons containing CpG sites that are significantly mutated in human bladder cancer (Figure 2). Codon 273, a major mutational hotspot in lung cancer of smokers, is a preferential site for BPDE binding in the unmethylated *p53* sequence, and cytosine methylation dramatically enhances BPDE binding at this site and makes it the strongest binding site for BPDE in the methylated *p53* sequence (Figure 7A-c and 7B-c). The results also show that cytosine methylation has no significant effect on the binding of N-OH-4-ABP at the regions surrounding CpG sequences, such as codons 280 and 285; nonetheless, codon 285 remains one of the preferential binding sites for N-OH-4-ABP in the methylated exon 8 sequence of the *p53* gene. The results in Figure 7 also show that C5 cytosine methylation at CpG sites has less of an enhancing effect on DNA binding for N-OH-4-ABP as compared to BPDE. After C5 cytosine methylation, there is a 2−5-fold enhancement of BPDE binding at methylated CpG sites compared to a 1−2-fold enhancement of N-OH-

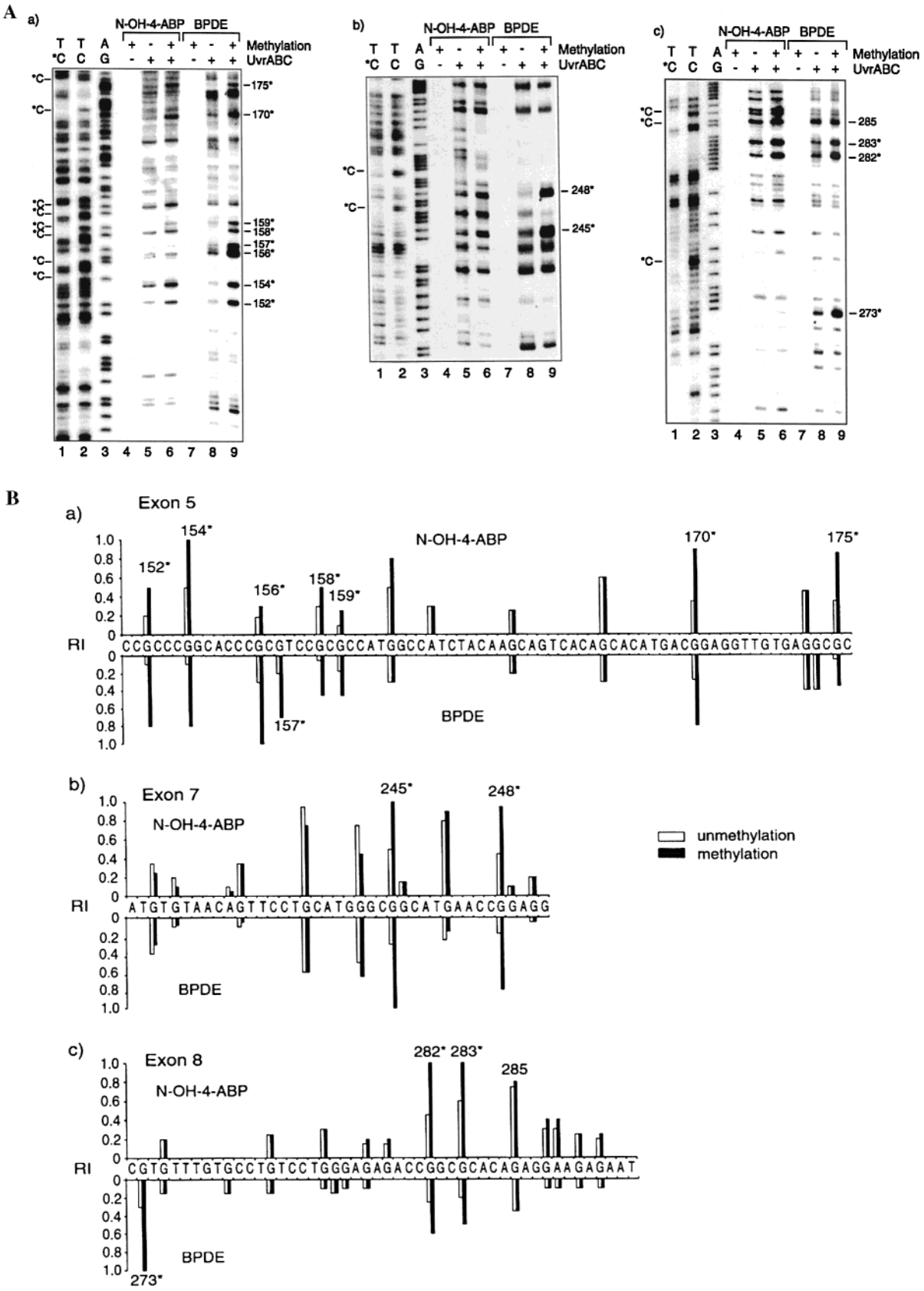

FIGURE 7: Effect of C5 cytosine methylation at CpG dinucleotides on the binding of N-OH-4-ABP and BPDE in exons 5, 7, and 8 of the human *p53* gene. The 5′-^{32}P-end-labeled DNA fragments containing exons 5 (A-a and B-a), 7 (A-b and B-b), and 8 (A-c and B-c) of the human *p53* gene were treated with *Sss*I and SAM to methylate the cytosines at the CpG sites. DNA fragments, with or without methylation treatment, were then modified with N-OH-4-ABP (30 μM) or BPDE (1 μM), reacted with UvrABC nuclease, and separated by denaturing gel electrophoresis. (A) Typical autoradiographs. The codon number of the bands corresponding to CpG sites or sites of interest is indicated. *C represents the methylated cytosine. (B) Quantitation of the effect of cytosine methylation at CpG sites on binding of N-OH-4-ABP (upper panel) and BPDE (low panel). The intensity of UvrABC incision bands was quantified with a PhosphorImager, normalized by the amount of DNA applied in the gel, and represented by the relative intensity (RI) of UvrABC incision.

4-ABP binding. This difference is clearly evident at codons 157 and 158 of exon 5, codons 245 and 248 of exon 7, and codon 273 of exon 8, which correspond to the mutational hotspots in lung cancer of smokers.

DISCUSSION

Thirty to sixty percent of human bladder cancers have a mutation in the *p53* gene (*15*, *16*). The *p53* mutational spectrum of bladder cancer bears the unique feature that codons 280 and 285 are mutational hotspots; these two codons do not contain CpG sites and are unique mutational hotspots in bladder cancer and cancers of other urinary organs. Codons 175, 248, and 273 all contain CpG sites, and are the common mutational hotspots in many human cancers including bladder cancer (IARC *P53* mutation database; Figure 2). Since 4-ABP plays a major role in human bladder carcinogenesis, the unique *p53* mutational feature in bladder cancer raises a possibility that metabolically activated 4-ABP may have an unusual DNA binding specificity in the *p53* gene of bladder cells. This important question remained unsolved because of lack of methodology to determine the 4-ABP-DNA binding specificity at the nucleotide sequence level. In this study, our results clearly show that *Escherichia coli* UvrABC nuclease, a nucleotide excision repair enzyme, incises 7 bases 5′ and 4 bases 3′ of N-OH-4-ABP-DNA adducts. The kinetics of incision at different sequences in a DNA fragment are the same, and the extent of UvrABC incision is proportional to the N-OH-4-ABP concentration. These results demonstrate that UvrABC nuclease is able to incise N-OH-4-ABP-DNA adducts specifically and quantitatively. This finding allowed us to map the N-OH-4-ABP binding spectrum in the human *p53* gene at nucleotide sequence level. Although the current study was confined to naked *p53* DNA fragments, several of our results are very revealing. First, codon 285 is a preferential site for N-OH-4-ABP binding, which suggests that mutations at this codon in bladder cancer are likely caused by the binding of this carcinogen. Second, C5 cytosine methylation at CpG sites greatly enhances N-OH-4-ABP binding at codons 175 and 248, two mutational hotspots in human bladder cancer, and these become the preferential binding sites for N-OH-4-ABP only after methylation. Third, regardless of methylation status, N-OH-4-ABP does not bind at codon 273, which suggests that etiological agents other than 4-ABP may be responsible for inducing mutation at this spot in human bladder cancer. Fourth, C5 cytosine methylation at CpG sites has less of an enhancing effect on DNA binding for N-OH-4-ABP as compared to BPDE. The results in Figure 7 show that after C5 cytosine methylation, there is a 2−5-fold enhancement of BPDE binding at methylated CpG sites compared to a 1−2-fold enhancement of N-OH-4-ABP binding. The different extent of DNA binding by N-OH-4-ABP and BPDE at methylated CpG sites may contribute to the fact that mutational hotspots in the *p53* gene in bladder cancer are not concentrated at CpG sites, while the mutational hotspots in the same gene in lung cancer of cigarette smokers preferentially occur at only CpG sites.

It is intriguing that, in contrast to other bulky chemical carcinogens such as BPDE, BCDE, and AFB1-DE, which bind strongly at methylated codon 273 (*19*−*22*), N-OH-4-ABP does not bind at codon 273 and C5 cytosine methylation does not enhance its binding at this sequence. Our previous results have shown that NAAAF also shows weak binding at this codon (*22*). Both NAAAF and N-OH-4-ABP bind guanine at the C8 position, while BPDE and BCDE bind guanine at the exocyclic N^2-amine and AFB1-DE at the N7 position. Perhaps, due to structural reasons, 4-ABP cannot bind favorably at codon 273 of the *p53* gene; therefore, mutations at this codon in human cancer are most likely induced by carcinogens other than 4-ABP.

Since the current study is limited to using naked *p53* DNA fragments, it is conceivable that the in vivo 4-ABP-DNA binding spectrum may be different from the in vitro binding spectrum due to the effects of chromatin structure, nuclear protein association, and gene activity, and it is likely that these factors may also affect the repair of the DNA adducts. These factors may be the reasons why we observed high N-OH-4-ABP binding in naked *p53* DNA at mutational cold spots such as codons 154, 161, 170, 246, and 283 (Figure 7). Under normal cellular conditions, the *p53* gene is in a proper genomic context, i.e., with a chromosomal structure, and either these codons may have low affinity toward N-OH-4-ABP and/or 4-ABP-DNA adducts formed at these sites may be efficiently repaired. It is reasonable to expect that the UvrABC nuclease incision method in combination with ligation-mediated polymerase chain reactions (*19*−*21*) will provide a sensitive tool to map the in vivo distribution of 4-ABP-DNA adducts in the *p53* gene and any other genes of interest at the nucleotide sequence level. The results from these studies may allow a better understanding of the role of 4-ABP in human bladder cancer and lead to the identification of other etiological agents of human bladder cancer based on their DNA binding specificity.

ACKNOWLEDGMENT

We thank Drs. O. Bhanot and Yen-Yee Tang for their critical review of the manuscript.

REFERENCES

1. Schulte, P. A., Ward, E., Boeniger, M., and Mills, B. (1988) in *Carcinogenic and Mutagenic Responses to Aromatic Amines and Nitroarenes* (King, C. M., Romano, L. J., and Schuetzle, D., Eds.) pp 23−25, Elsevier, New York.
2. Vineis, P. (1994) *Environ. Health Perspect. 102 (Suppl. 6)*, 7−10.
3. Beland, F. A., Beranek, D. T., Dooley, K. L., Heflich, R. H., and Kadlubar, F. F. (1983) *Environ. Health Perspect. 49*, 125−134.
4. Poirier, M. C., Fullerton, N. F., Smith, B. A., and Beland, F. A. (1995) *Carcinogenesis 16*, 2917−2921.
5. al-Atrash, J., Zhang, Y. J., Lin, D., Kadlubar, F. F., and Santella, R. M. (1995) *Chem. Res. Toxicol. 8*, 747−752.
6. Underwood, P. M., Zhou, Q., Jaeger, M., Reliman, R., Pinney, S., Warshawsky, D., and Talaska, G. (1997) *Toxicol. Appl. Pharmacol. 144*, 325−331.
7. Talaska, G., al-Juburi, A. Z. S. S., and Kadlubar, F. F. (1991) *Proc. Natl. Acad. Sci. U.S.A. 88*, 5350−5354.
8. Bartsch, H., Malaveille, C., Friesen, M., Kadlubar, F. F., and Vineis, P. (1993) *Eur. J. Cancer 29A*, 1199−1207.
9. Curigliano, G., Zhang, Y. J., Wang, L. Y., Flamini, G., Alcini, A., Ratto, C., Giustaachchini, M., Alcini, E., Cittadini, A., and Santella, R. M. (1996) *Carcinogenesis 17*, 911−916.
10. Martone, T., Airoldi, L., Magagnotti, C., Coda, R., Randone, D., Malaveille, C., Avanzi, G., Merletti, F., Hautefeuille, A., and Vineis, P. (1998) *Int. J. Cancer 75*, 512−516.
11. Romano, G., Garagnani, L., Boninsegna, A., Ferrari, P., Flamini, G., De Gaetani, C., Sgambato, A., Giovanni, F.,

Curigliano, G., Ferretti, G., Cittandini, A., and Trentini, G. (1999) *Anticancer Res. 19*, 4571−4576.
12. Kadlubar, F. F., Beland, F. A., Beranek, D. T., Dooley, K. L., Heflich, R. H., and Evans, F. E. (1982) in *Environmental Mutagens and Carcinogens* (Sugimura, T., Kondo, S., and Takebe, H., Eds.) pp 388−396, Alan R. Liss, New York.
13. Kadlubar, F. F., Dooley, K. L., Teitel, C. H., Roberts, D. W., Benson, R. W., Butler, M. A., Bailey, J. R., Young, J. F., Skipper, P. W., and Tannenbaum, S. R. (1991) *Cancer Res. 51*, 4371−4377.
14. Badawi, A. F., Hirvonen, A., Bell, D. A., Lang, N. P., and Kadlubar, F. F. (1995) *Cancer Res. 55*, 5230−5237.
15. Greenbaltt, M. S., Bennett, W. P., Hollstein, M., and Harris C. C. (1994) *Cancer Res. 54*, 4855−4878.
16. Hollstein, M., Shomer, B., Greenblatt, M., Soussi, T., Hovig, E., Montesano, R., and Harris, C. C. (1996) *Nucleic Acids Res. 24*, 141−146.
17. Pfeifer, G. P., and Denissenko, M. F. (1998) *Environ. Mol. Mutagen. 31*, 197−205.
18. Hainaut, P., and Pfeifer, G. P. (2001) *Carcinogenesis 22*, 367−374.
19. Denissenko, M. F., Pao, A., Tang, M.-s., and Pfeifer, G. P. (1996) *Science (Washington, D.C.) 274*, 430−432.
20. Smith, L. E., Denissenko, M. F., Bennett, W. P., Li, H., Amin, S., Tang, M., and Pfeifer, G. P. (2000) *J. Natl. Cancer Inst. 92*, 803−811.
21. Denissenko, M. F., Chen, J. X., Tang, M.-s., and Pfeifer, G. P. (1997) *Proc. Natl. Acad. Sci. U.S.A. 94*, 3893−3898.
22. Chen, J. X., Zheng, Y., West, M., and Tang, M.-s. (1998) *Cancer Res. 58*, 2070−2075.
23. Sancar, A., and Sancar, G. B. (1988) *Annu. Rev. Biochem. 57*, 29−67.
24. Van Houten, B. (1990) *Microbiol. Rev. 54*, 18−51.
25. Sancar, A., and Tang, M.-s. (1993) *Photochem. Photobiol. 57*, 905−921.
26. Grossman, L., and Yeung, A. T. (1990) *Mutat. Res. 236*, 213−221.
27. Tang, M.-s. (1996) in *Technologies for Detection of DNA Damage and Mutations* (Pfeifer, G., Ed.) pp 139−153, Plenum Press, New York.
28. Tang, M.-s., Pierce, J. R., Doisy, R. P., Nazimiec, M. E., and MacLeod, M. C. (1992) *Biochemistry 31*, 8429−8436.
29. Chen, J. X., Pao, A., Zheng, Y., Ye, X., Kisleyou, A. S., Morris, R., Slaga, T. J., Harvey, R. G., and Tang, M. (1996) *Biochemistry 35*, 9594−9602.
30. Beland, F. A., Doerge, D. R., Churchwell, M. I., Poirier, M. C., Schoket, B., and Marques, M. M. (1999) *Chem. Res. Toxicol. 12*, 68−77.
31. Thomas, D. C., Levy, M., and Sancar, A. (1985) *J. Biol. Chem. 260*, 9875−9883.
32. Sancar, A., and Rupp, W. D. (1993) *Cell 32*, 249−260.
33. Maxam, A. M., and Gilbert, W. (1980) *Methods Enzymol. 65*, 499−560.
34. Tornaletti, S., and Pfeifer, G. P. (1995) *Oncogene 10*, 1493−1499.
35. Church, G. M., and Gilbert, W. (1984) *Proc. Natl. Acad. Sci. U.S.A. 81*, 1991−1995.

BI020093S